Contrasting uncertainties in estimating floods and extreme low flows

Hadush Meresa[1] and Yongqiang Zhang [1*]

[1]Key Laboratory of Water Cycle and Related Land Surface Processes, Institute of Geographic Sciences and Natural Resources Research, Chinese Academy of Sciences, Beijing 100101, China

* Corresponding author: Yongqiang Zhang

Email: yongqiang.zhang2014@gmail.com; zhangyq@igsnrr.ac.cn

Key points:

- A comprehensive uncertainty estimation approach developed for hydrological extremes
- It quantifies four uncertainty sources from inputs to hydrological extreme distributions
- Individual source of uncertainty separated from the total source of uncertainty
- Flood magnitude and frequency controlled by input data and frequency distribution
- Low flow magnitude and frequency dominated by model types and parameters

Abstract

The accuracy and reliability of river flow model predictions and hydrological extreme frequencies are influenced by different sources of uncertainties that results from the input variables, conceptual model structures, model parameters, and extreme frequency distributions. Therefore, evaluation and quantification of possible sources of uncertainty and their influence on water resource planning and extreme management is very important for risk modeling and extreme hydrological management. The main objective of this research work is to identify and holistically address the uncertainty propagation from the input data to frequency of hydrological extremes. This includes to identify and estimate their contribution to flood and low flow magnitude by using two objective functions in flood (NSE) and low flow (LogNSE) modeling, three hydrological models (XAJ, HBV, and GR8J), 50, 000 hydrological parameter sets and five frequency distribution models (LN, Pearson-III and GEV). The influence of uncertainty on the simulated flow is not uniform across all the selected eight catchments due to different flow regimes and mechanism for runoff generation. Uncertainty in the modeling of extreme high flow frequency mainly comes from the quality of the input data, while in the modeling of low flow frequency, the main contributor to the total uncertainty is from model parameterization. This result is also confirmed by using the Analysis Of Variance Analysis (ANOVA) that considers additional information about the interaction impact of the main factors. The total uncertainty of QT90 (extreme peak flow quantile at 90-year return period) quantile shows the interaction of input data and extreme frequency models has significant influence on the total uncertainty. In contrast, in the QT10 (extreme low flow quantile at 10-year return period) estimation, the hydrological models and hydrological parameters have significant impact on the total uncertainty. This implies that the four factors and their interactions may cause significant risk in water resource management and flood and drought risk management, and neglecting of these four factors and their interaction in disaster risk management, water resource planning and evaluation of environmental impact assessment is not feasible and may lead to big risk.

Key works: uncertainty, GLUE, ANOVA, hydrological model, extremes, frequency

1. Introduction

Numerous hydrological river flow models are used to characterize, understand and forecast surface water flow under both climatic and land use influences to provide valuable information for water resources management and planning, risk analysis and decision making. The accuracy and reliability of river flow predictions are essential for water extreme management, policy making and water allocation as well as integrated and sustainable water resource management practices (disaster management, irrigation water management, hydropower regulation, ecological water requirement) (Meresa and Romanowicz, 2017; Meresa and Gatachew, 2018; Meresa, 2019; Okoli et al., 2019). The precision and trustworthiness of river flow model predictions and extreme frequencies are influenced by different sources of uncertainty that results from hydrological model input variables (such as temperature and precipitation) (Kavetski et al., 2006; Bae et al., 2018), conceptual model structures (Dams et al., 2015 ; Mockler et al., 2016; Vetter et al., 2017), model parameters, and extreme frequency distributions (Meresa and Romanowicz, 2017). Defining and estimation of the critical uncertainty sources at each stage from input data to frequency of hydrological extremes is important to have comprehensive understanding on the role of systematic and inherent errors. The nonlinear and inerasable character of uncertainty propagation requires to contrasted at each stage of uncertainty level that starts from the model input (precipitation and temperature) to the low flow and flood frequencies for better water extreme management and infrastructure construction (e.g. dam, dyke, bridge, flood control structures).

defining and estimation of uncertainty in water resource planning and extreme management is very important in risk modeling and extreme hydrological events, and is identified by hydrological community as one of the 23 unsolved problems in hydrology (Blöschl et al., 2019). Numerous water resource and hydrologic researchers have attempted to identify different sources of uncertainty in water resources and hydrological extreme frequencies (Vrugt et al., 2008; Xu et al., 2010; Chen et al., 2013; Vetter et al., 2017; Zhang et al., 2016; Qi et al., 2016; Meresa and Romanowicz, 2017; Sun et al., 2017; Bae et al., 2018; Hattermann et al., 2018 ; Kusangaya et al., 2018; Prein, 2019; Her et al., 2019). These research works have addressed uncertainty in water resources and hydrological extreme modeling in the isolated form, and requires to contrasting the critical sources in projected high and low flow. For example, Kavetski et al. (2006) examined input uncertainty in hydrological modeling using a Bayesian approach in two catchments in North America. Her et al. (2019) branded the sources of uncertainty using Analysis Of Variance Analysis (ANOVA) and come up with the hydrological structure and parameters and climate change has significant contribution to hydrological extreme condition. They strongly recommended to incorporate input uncertainty in Ohio river basin. Chen et al. (2013) considered hydrological model structure and hydrological parameter uncertainty in their uncertainty analysis using GLUE approach, and found that the three sources has significant contribution to the high flow in China. Prein, (2019) stated that the extreme precipitation events and its implication of intense hydrologic cycle could highly expose to uncertainty. Similarly, Sun et al. (2017) identified multiple sources of uncertainty (distribution types, distribution parameters and peak over threshold) in flood frequency and found that distribution types could play a major role in controlling the flood magnitude. Zhang et al. (2016) also did uncertainty investigation in snow dominated catchments from China and found that input uncertainty is greater than hydrological parameters in peak flow estimation. others have investigated input and hydrological parameters (e.g Zhang et al., 2016; Bae et al., 2018), hydrological parameters and model structure (e.g. Butts et al., 2004; Jin et al., 2010), climate change and hydrological parameters (e.g. Krysanova et al., 2018; Her et al., 2019; Meresa, 2019), climate change and flood frequency (e.g. Qi et al., 2016a; Meresa and Romanowicz, 2017), distribution parameters and types (e.g. Sun et al., 2017). These studies have shown that only one aspect of systematic and/or inherent uncertainty is not enough to address the problem in estimation of extreme flow. However, it is not widely studied the contrasting of uncertainty propagation at stage and level from input data to frequency of hydrological extremes (flood and low flow) (Marton and Paseka, 2017; Kiang et al., 2018). This uncertainty propagation comprises input data, hydrological model structure, hydrological parameters, and extreme probability distribution types, as well as, desired to analyze its effect on magnitude and frequency of extremes. the accuracy of meteorological variables can be impacted by systematic, instrumental errors and external factors (Mcmillan et al., 2011;Karakoram, 2016;Yen et al., 2018); parameter representation and instability of hydrological models may lead to significant error in timing and magnitude of hydrological process and regimes (Zhang et al., 2016; Meresa and Romanowicz, 2017; Bae et al., 2018); simplification of the real watershed processes is another source of error in water resource modeling (Song et al., 2015; Meresa and Gatachew, 2018) and difficult to represent in a single model, which is mainly due to the lack of precise mathematical principles, catchment heterogeneity and complexity of water cycle (Jiang et al., 2017; Emam et al., 2018); and the frequency-magnitude relationship is strongly influenced by distribution type and parameters (Ham et al., 2017), and only one extreme distribution may led to a certain level of uncertainty. Furthermore, there is no unique hydrological parameter sets, single hydrological structure that can represent different hydrological process represent, hydro-climatic and physiographic conditions due to non-stationerity and uniform high or low flow percentile distribution and can have an error in distribution fitting (Hu et al., 2013; Sun et al., 2017; Winter, 2018).

The main objective of this research work is to identify and address the critical uncertainty sources in extreme flow modeling under using variety plausible rainfall characteristics and combine with hydrological parameters and structures to assess extreme frequency using different distributions. This combines statistical climate ensembles, multiple parameter sets for three conceptual hydrological model structure and five flood frequency distribution models to investigate the interplay among the associated uncertainty in flood and low flow modeling, i.e calibration of conceptual hydrological models using two objective functions for high and low flow, three hydrological models, 50,000 hydrological parameter sets and five frequency distribution models.

Following this part, section 2 describes in detail about the study river basins and datasets, section 3 presents the methods and numerical modeling experiments. Results and detail discussion are presented in section 4. Finally, in section 5 the main conclusions are summarized.

2. Study river basins and datasets

To avoid the human intervention effect on flow prediction, eight medium sized natural river catchments (unregulated and unurbanized) were selected from four countries for estimation of uncertainty propagation from input to frequencies of hydrological extremes modeling. These eight river basins are located in different hydro-climatic and physiographic conditions: in Poland (C1P: Nysaklodska and C2P: Dunajec catchments), Norway (C1N: Viksvaten and C2N: Fustvatn catchments), Ethiopia (C1E: Hombole and C2E: Awash Bello catchments), and China (C1C: Gaoshiya and C2C: Hanjiamou catchments) (Figure 1). The selected case study catchments vary in climate regime, drainage density, river length, catchment area and shape, topography, soil type, surface and subsurface properties and land use land cover type. Each has been the focus of many hydrologic investigations (e.g. Feng et al., 2016; Meresa et al., 2017; Meresa and Gatachew, 2018). streamflow properties of these eight catchments are summarized in Table 1. of the selected catchments, Awash bello from Ethiopia and Gaoshiyo from China have zero m^3/s flow in their tenth percitile value. while, the median (Q50) shows very low flow value (0.26 m^3/s and 0.34 m^3/s, respectively) in these catchments. This may happen and is commonly seen in ephemeral watersheds.

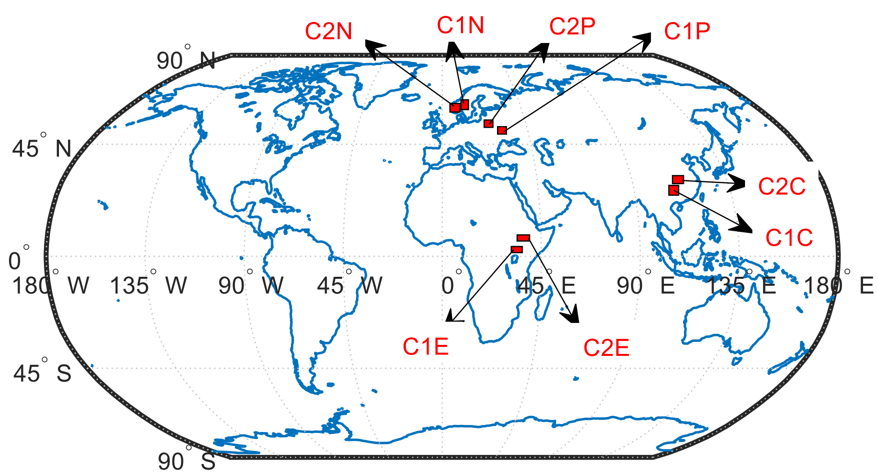

Figure 1. location of study areas

The observed time series of precipitation, temperature and streamflow data were collected from their respective country offices. The length and quality of available meteorological and hydrological record is good; 30+ years of recorded data from 1973 to 2018, from which the first 20 years recorded data was used for calibration and the remaining nine years recorded data for validation of three hydrological models. Daily potential evapotranspiration for each catchment was estimated by using a temperature-based technique (Hamon, 1963).

Table 1. Statistical description of observed streamflow

Code: Name	Area [Km^2]	Log/Lat	Q10 [m^3/s]	Q50 [m^3/s]	Q95 [m^3/s]	CV [-]	Time period
C1P: Nysaklodska	1061.5	16.65/50.43	4.58	9.00	33.6	0.86	1973-2009
C2P: Dunajec	681.1	20.03/49.48	4.30	10.00	37.3	0.88	1973-2009
C1E: Hombole	7656.2	38.783/8.383	3.17	8.40	212.97	0.56	1988-2018
C2E: Awash Bello	2566.1	38.416/8.85	0.01	0.26	14.24	0.29	1988-2018
C1N: Viksvatn	508.1	5.886/61.333	6.79	34.00	118.97	1.19	1974-2009
C2N: Fustvatn	525.7	13.308/65.905	4.73	24.02	101.81	1.04	1974-2009
C1C: Gaoshiya	1252.1	111.05/39.0	0.01	0.34	4.93	0.73	1973-2012
C2C: Hanjiamou	2452.1	109.15/38.0	1.32	2.63	4.00	0.13	1973-2012

*Note: C1P represents catchment one from Poland, C2P catchment two from Poland, C1E catchment one from Ethiopia, C2E catchment one from Ethiopia, C1N catchment two from Norway, C2N catchment one from Norway, C1C catchment one from China, and C2C catchment one from China.

3. Modeling and numerical methods

The uncertainty propagation from input to extreme hydrological condition was conducted using three conceptual hydrological models (Xinanjiang (simplified as XAJ thereafter) (Zhao, 1992), HBV (Bergstrom, 1976) and GR8J ((Perrin et al., 2003))), five distribution models (LN, Pearson-III, GEV, Gamma and Exponential) and 50,000 hydrological parameter sets using Monte-Carlos simulation (Figure 2). Realizations of 1,000 precipitation and temperature time series generation using statistical approach for input data uncertainty band estimation, sampling of 50,000 hydrological parameters sets via MCS-GLUE for hydrological parameter uncertainty band estimation (Beven and Binley, 1992), three conceptual hydrological models (XAJ, HBV and GR8J) for hydrological model structure impact understanding and to estimate the extreme frequency of peak and low flow by applying five different frequency distribution models (Figure 5).

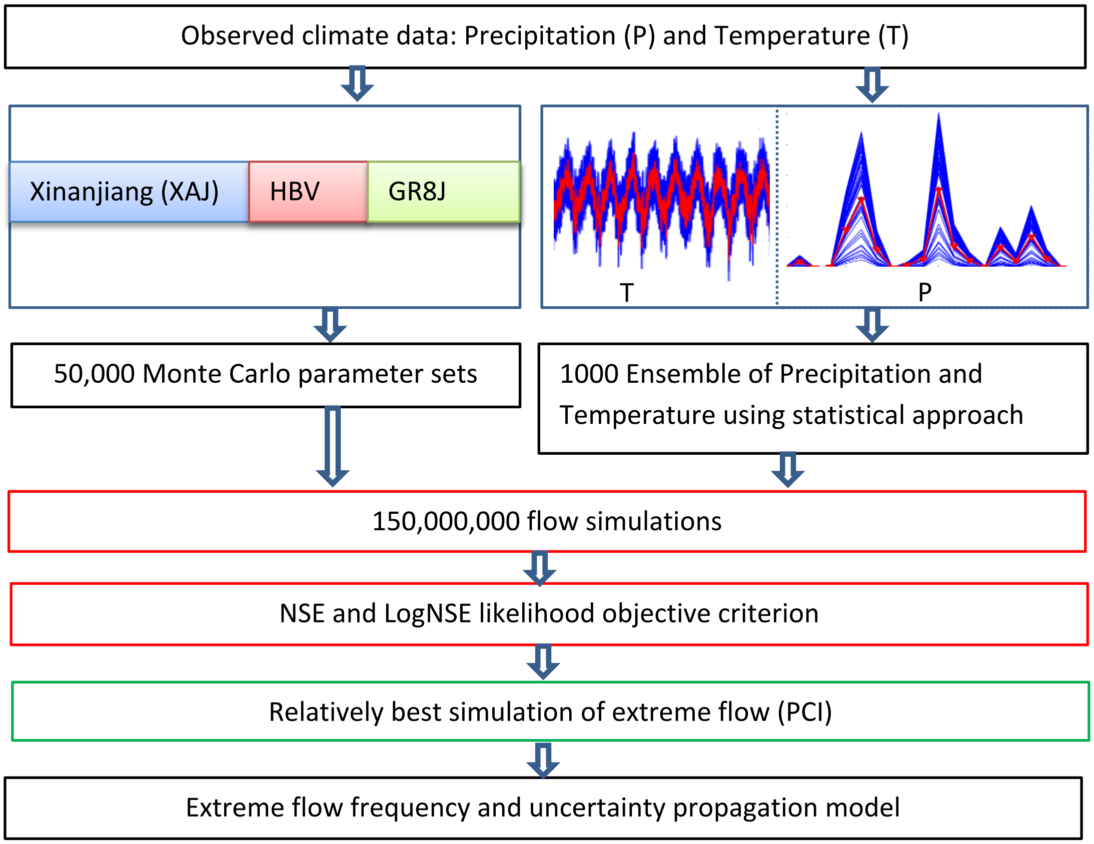

Figure2. The research flow chart of this study

3.1 Precipitation and temperature ensemble generation/modeling

Precipitation and temperature variables are the main drivers of hydrological simulations. Climate variables play a key role in hydrological process and are highly varied with time and space. of which, temperature and precipitation are associated with the pattern of regional and local atmospheric circulations (Kidd and Huffman, 2011; Wu et al., 2011; Mockler et al., 2016). In recent decades, various advanced statistical and stochastic approaches have been developed for climate predictions by incorporating the seasonal and annual fluctuations (Wu et al., 2011; Jones et al., 2013; Khazaei and Ahmadi, 2013; Breinl et al., 2017). These studies were highly exposed uncertainty due to complex stochastic approach (Vesely et al., 2019) and number of parameters (Breinl et al., 2017; Okoli et al., 2019).

In this study, input data, such as precipitation and temperature were used for forcing the three conceptual hydrological models. For the input uncertainty analysis, the ensemble realization of precipitation and temperature were generated using a statistical approach (equation (1) and equation (2)). The statistical approach that introduced in this study for generation of ensemble precipitation and temperature is as follows:

$$PPE_{n,j} = PPO_n * EPE_{n,j}\ ; \quad where\ \ EPE_{n,j} \approx N(0.01, \sigma_p^2) \qquad (1)$$

$$TTE_{n,j} = TTO_n + ETE_{n,j}\ ;\quad where\quad ETE_{n,j}\ \approx N(\mu_t, \sigma_t^2) \tag{2}$$

where n represents a simulation at specific time and j denotes the jth ensemble of realizations. $PPE_{n,j}$ and $TTE_{n,j}$ represent the number of ensemble of precipitation and temperature realization at time n, respectively. TTO_n and PPO_n symbolize the observed precipitation and temperature at time n, respectively. The $EPE_{n,j}$ and $ETE_{n,j}$ represent the possible ensemble of errors variability range of generated precipitation and temperature at time n, respectively.

Monte Carlo simulation with Gaussian distribution sampling was used to sample 1000 precipitation and temperature ensemble of realizations by multiplying (high variability nature) and adding (less variability) noise term $EPE_{j,n}$ and $ETE_{j,n}$, to observed precipitation and temperature recorded data, respectively (Ajami et al., 2007). The observed climate variables are perturbed at a given time by the error terms derived from the Gaussian distribution with constant mean and standard deviation, $N(0.01, \sigma_p^2)$ and $N(\mu_t, \sigma_t^2)$ for precipitation and temperature, respectively.

3.2 Hydrological extreme modeling

Three hydrological models were considered to investigate the impact of hydrological model structures on the hydrological extremes. The three hydrological models (XAJ, HBV and GR8J) used daily precipitation and daily temperature as input to simulate runoff at the outlet of the catchment.

The Hydrologiska Byråns Vattenbalansavdelning (HBV) (Bergstrom, 1976) is widely applied in different hydro-climate condition of the world (Meresa et al., 2017; Meresa and Gatachew, 2018; He et al., 2018b). HBV is mainly designed to simulate streamflow using precipitation, temperature and evapotranspiration (Bergstrom, 1976). Catchment forest status and elevation of precipitation station (or centroid elevation) are also used. The HBV model structure used in this study has three storage reservoirs in snow routing, soil moisture, and sub-surface routing to characterize river flow. The model has fourteen parameters set to control the input and output catchment process (Table 2). Génie Rural à 8 paramètres Journalier (GR8J) (Perrin et al., 2003) is a daily lumped conceptual hydrological model with eight parameters and applied in many parts of the world (Meresa et al., 2017;Meresa and Gatachew, 2018). GR8J was used with eight hydrological parameters (Table 2). GR8J model structure has two consecutive stores: one relates to runoff production and the other associates to routing store package. Daily precipitation and daily evapotranspiration are the main climate variables. The detailed information about the model is described in Perrin et al. (2003). The Xinanjiang (XAJ) hydrological model is also used to simulate streamflow in different hydro-climatic zones of the world (Zhao, 1992). It is a daily conceptual hydrological model and consists of three runoff generation packages. The conceptual structure is governed by fourteen hydrological parameters (Table 2). Like HBV and GR8J, the XAJ model requires daily precipitation and evapotranspiration to simulate streamflow at the outlet of the catchment.

Table 2 A Range of hydrological parameters of XAJ, HBV and GR8J models. L stands for Lower value and U for upper part of the model parameters

Model	parameter	description	HBV L	HBV U
XAJ	SM	the free water capacity of the surface soil layer	5	100
	KG	outflow coefficients of the free water storage to groundwater	0.5	0.65
	KSS_KG	daily recession constant of groundwater storage	0.7	0.8
	KKG	outflow coefficients of the free water storage to interflow	0.05	0.8
	KKSS	recession constant of the lower interflow storage	0.05	0.8
	WUM	water capacity in the upper soil layer	10	400
	WLM	water capacity in the lower soil layer	10	400
	WDM	Water capacity in the deeper soil layer	10	400
	IMP	recession constant for channel routing	0.005	0.8
	B	exponent of the tension water capacity curve	0.05	0.6
	C	coefficient of deep evapotranspiration	0.05	0.3
	EX	exponent of the free water capacity curve	0.5	5
	XE	Flow proportion factor	0	0.5
	KE	Slot storage coefficient	0.5	10
HBV	FC	Maximum soil storage	0.1	250
	BETA	Shape coefficient	0.01	5
	LP	threshold for reduction of evaporation	0.1	2
	ALPHA	Measure for non-linearity of flow in quick runoff	0.1	0.6
	KF	Recession coefficient for runoff from quick runoff	0.005	0.6
	KS	Recession coefficient for runoff from base flow	0.005	0.6
	PERC	Percolation rate occurring when water is available	0.01	400
	CFLUX	Rate of capillary rise	0.5	400
	TT	Temperature threshold for snowfall	-1	10
	TTI	Temperature threshold interval length	0.5	15
	CFMAX	Snowmelt rate	3	30
	FOCFMAX	correction to give a threshold temperature	0.6	2.6
	CFR	Refreezing	0.05	2.05
	WHC	Water holding capacity of snow	0.1	2.1
GR8J	TT	Temperature threshold for snowfall	-1	10
	TTI	Temperature threshold interval length	0.5	7.99
	CFMAX	Snowmelt rate	3	20
	CFR	Refreezing	0.05	2.1
	X1	production store capacity [mm]	200	229.05
	X2	Inter-catchment exchange coefficient [mm/d]	0	1.6
	X3	routing store capacity [mm]	10	46.77
	X4	unit hydrograph time constant [d]	0	1.98

The upper and lower limits of the three hydrological models are listed in Table 2.

3.3 hydrological model parameter selection and evaluation

There are different ways of parameter sampling from the upper and lower boundary of hydrological parameters, which depends on the computing times and number of parameters in a specific hydrological model. Beven and Binley, (2014) stated that there is no fixed threshold in parameter sampling that varies from thousand to hundred thousand of parameters sets. In this study, 50,000 parameter sets were generated from each GR8J, HBV, XAJ hydrological model parameters range. High flow and low flows have different characteristics, and need two objective functions for calibration . Meresa and Romanowicz, (2017) stated that NSE likelihood function is good for high flow simulation due to the interest on peak flow and LogNSE for low flow. In this study, two objective functions were used to simulate both flow regimes (high and low flow regimes) and evaluated against observed streamflow. NSE, objective function is for high flow simulation and LogNSE for low flow simulation. Based on the performance of each model, 200 sets of simulations for each hydrological model and data input were selected as behavioral condition.

$$NSE = 1 - \frac{\sum_{t=1}^{j}(Q_{o,t}-Q_{m,t})^2}{\sum_{t=1}^{j}(Q_{O,t}-\bar{Q}_O)^2} \quad \text{and} \quad LogNSE = 1 - \frac{\sum_{t=1}^{j}(\log(Q_{o,t})-\log(Q_{m,t}))^2}{\sum_{t=1}^{j}(\log(Q_{O,t})-\overline{\log(Q_{o,t})})^2} \qquad (3)$$

where Qo,t and Qm,t are observed and simulated flow at time t, Qo is the mean observed flow and j is the length of the time series. For each hydrologic model, the best values of NSE and LogNSE are selected for hydrological model structure and parameter uncertainty analyses.

3.4 Evaluation of ensemble simulations

In this research work, the ensemble of simulations was evaluated using the proportion of extreme flow inside 95% confidence intervals (PCI) principle. Two hydrological extremes, peak and low flow were used and evaluated by the derived CI. This is very helpful to identify (fix threshold) the behavioral and non-behavioral simulations, and to select the best threshold value of NSE and LogNSE. According to Li et al. (2011) and Xu, (2014), PCI way of ensemble evaluation is more reliable and efficient in uncertainty analysis.

$$PCI = \left[1 - \left|\left(\frac{NQ_{i,p}}{T} - 0.95\right)\right|\right] * \frac{1}{T} * [(\sum \frac{L_{u,t,p}-L_{l,t,p}}{Q_{o,t}})] \qquad (4)$$

where $L_{L,t,p}$ and $L_{U,t,p}$ are the lower and upper boundary values of the extreme flow at time t and portion p, T is the sum of time steps, $Q_{o,t}$ is the observed extreme flow at t time step, $NQ_{in,p}$ is the number of extreme flow observations which lie within the extreme flow CI. The PCI is used in 95% CI evaluation, which ranges from zero to infinity values (Li et al., 2011). The shape of the 95% CI is governed by the value of PCI; if PCI is closer to 0.95 it means more of the observed time series extreme fall in the confidence interval band.

Zero flows were commonly observed in the low flow analysis and handled by setting the low boundary of PCI is zero, whereas the upper part of the PCI is calculated using equation (4).

3.5 Extreme Frequency Analysis (EFA)

Extreme frequency analysis is very crucial to understand the probability of occurrence of floods and/or low flows various distributions have been to estimate these frequencies. For example the Log-Pearson III distribution model is very popular in the USA and Australia for infrastructure design (Griffis and Stedinger, 2007), General Extreme Value and Pearson Type III are used in Europe (Madsen et al., 2013) and the Wakeby and Log-Normal distributions have been frequently used in Asian countries (Chen et al., 2013). a single distribution model may not be able to capture the entire temporal and spatial variability of hydrological extremes. Therefore, in extreme frequency uncertainty analysis, five common distribution types (LN, Pearson-III, GEV) applied across the world in extreme frequency modeling. Those distributions were fitted to annual maximum flow and annual seven days minimum flow in order to understand hydrological flood and low flow in the selected eight catchments from Poland, Norway, Ethiopia, and China. In equations (5)-(9), the respective probability density function (PDF) of each distribution is presented. Exponential distribution is a simple model with one parameter; whereas, LN and Gamma has two parameters and GEV has three parameters. In this research, one-two-three parameter distributions were considered.

Log-Normal $$f(x) = \frac{\exp(-\frac{1}{2}\left(\frac{lnx-\mu}{\sigma}\right)^2)}{x\sigma\sqrt{2\pi}} \qquad \sigma, \mu\ (\sigma>0) \tag{5}$$

Pearson-III $$f(x) = \frac{(x-\gamma)^{\alpha-1}}{\beta^{\alpha}\Gamma(\alpha)}\exp(-\frac{x-\gamma}{\beta}) \qquad \alpha, \beta, \Upsilon\ (\alpha>0, \beta>0) \tag{6}$$

GEV $$f(x) = \begin{cases} \frac{1}{\sigma}\exp(-(1+kz)^{\wedge-\frac{1}{k}})(1+kz)^{-1-\frac{1}{k}} & k \neq 0 \\ \frac{1}{\sigma}\exp(-z-exp(-z)) & k = o \end{cases} \qquad K, \sigma, \mu\ (\sigma>0) \tag{7}$$

3.6 Generalize Likelihood Uncertainty Estimation (GLUE)

The Generalize Likelihood Uncertainty Estimation (Beven and Binley, 1992) approach is widely applied to quantify different sources of uncertainty in hydrological modeling (Mockler et al., 2016; Meresa and Romanowicz, 2017; Bae et al., 2018). GLUE is based on Monte Carlo (MC) simulations and the behavioral condition of the parameter sets is controlled by the chosen objective function. GLUE focuses on reasonable possible solution generation from a large set of likelihood of sets using a nominal threshold, which defines best behavioral condition (Beven and Binley, 2014).

GLUE is a non-formal statistical approach that includes Monte Carlos simulations. The hydrological model runs using the entire space of hydrological parameter combinations and is evaluated by deploying goodness-of fit criterion (Beven, 2007). A likelihood function H(X) is used to separate the non-behavioral and behavioral simulations produced by different variables X, such as input data, hydrological model parameters, hydrological model structures, and extreme frequency models. Every i^{th} of the variable X has its own one likelihood measure at time t. The ensemble of each variable X_i (i=1…….m) provide the multi-likelihood measure values $H(X_i)$. The GLUE function is shown in Equation (8), where the standard deviation/ variance of residual σ^2_e value is the error in the estimated results affected by the model parameters/input data/hydrological model type/extreme frequency distribution models. If the estimated value of σ^2_e is near equal to the estimated maximum likelihood or equal to the standard deviation/variance of the observation data σ^2_o, the likelihood measure H(X) is equal to zero, which indicates extremely high uncertainty.

$$H(X) = 1 - \frac{\sigma_O^2}{\sigma_e^2} \tag{8}$$

In this study, GLUE was used to estimate the propagation of uncertainty from the input to extreme frequencies. GLUE was extended to quantify the uncertainty associated with hydrological parameters, input data, hydrological models and extreme frequencies.

The overall procedure and concept are presented in Figure 2.

3.7 Total and each uncertainty component estimation and combination methods

The cumulative uncertainty approach was applied to define the total uncertainty in extreme flood frequency modeling. Thus, first defines the aggregate uncertainty up to stage k=4 denoted by $U^{cum}(X_1 \dots .. X_k)$. Intuitively, the uncertainty due to hydrological model selection, the choice of input quality and type, hydrological parameter sets or flood frequency models, up to stage k=4 can be characterized as the variation in the extreme hydrological design values due to these four factors, and include a choice up to stage k, after stage are fixed. That is, the sum of uncertainty up to stage k=4 is defined as

$$U^{cum}(x_1, \dots, x_k) = \frac{1}{\pi_{j=k+1}^{nj}} \sum_{x_{k+1} \epsilon x_{k+1}} \dots \sum_{x_k \epsilon x_k} U(q_{x\ k+1 \dots\dots xk}) \tag{9}$$

As it is proven in the result section, one of the most fascinating estates of this uncertainty approach is that it keeps summing as the factor steps progress and type of the extreme hydrological values. That is, for most acceptable uncertainty measures of U, which $U^{cum}(x_1, \dots x_j) \leq U^{cum}(x_1., \dots x_k)$ for all j < k=4. More explicitly, as more k stages increase, more uncertainty is appeared the extreme hydrological design variable.

Since the aggregated uncertainty has an ascending character, each uncertainty defines at each successive stage and expressed as the difference between successive sum of uncertainties of each factor. That is, the uncertainty of stage k=4, denoted by $U^{cum}(X_k)$, can be described as

$$U^{cum}(X_k) = U^{cum}(X_1, \dots, X_k) - U^{cum}(X_1, \dots., X_{k-1}) \tag{10}$$

Note that each uncertainty at stage k=4 is a magnitude of contribution to the total uncertainty. Also, the sum of uncertainties of individual sources is always equal to the cumulated uncertainty $U^{cum}(X_1, \ldots, X_k)$.

3.8 Uncertainty decomposition

Four sources of uncertainty in extreme frequency analysis driving from input data, hydrological model structure, hydrological parameters and extreme frequency distribution models were estimated by means of variances decomposition approach (ANOVA). ANOVA can decompose the aggregated source of uncertainty into individual terms and their interactions (Meresa and Romanowicz, 2017). In this study, n-way ANOVA was used to distinguish the main variable effects and their interaction effect on the aggregated extreme frequency indices.

$$SST = SS_{ID} + SS_{HM} + SS_{HP} + SS_{EF} + SS_{IDHM} + SS_{IDHP} + SS_{IDEF} + SS_{HMHP} + SS_{HMEF} + SS_{HPEF} \quad (11)$$

where SST is the square sum of the total error, SSID is the sum of standard error of input data, SSHM stands for sum standard error of hydrological models, SSHP is the sum of standard of hydrological parameters, SSEF sum standard error of extreme frequency, SSIDHM is the sum of standard errors of combined effect of input data and hydrological models, SSIDEF is the sum of standard error of combined effect of input data and extreme frequency, SSHMHP is the sum of standard error of combined effect of hydrological models and hydrological parameters.

4. Results

4.1 Ensemble of input precipitation and temperature evaluation

Figure 3A, B evaluates the ensembles of input precipitation and temperature time series data with 95% confidence interval, respectively. The correlation of best 100 time series of daily precipitation (Figure 3A) and daily air temperature (Figure 3 B) was selected for further use in forcing of hydrological models and assess the input uncertainty. The generated ensemble of precipitation and temperature has shown very high correlation and the observed values are falls in the 95% of confidence interval. In fact, 95% confidence interval (CI) of the 100 groups of generated precipitation is much more highly correlated to observed data than the total ensembles. This indicates that the proposed statistical climate generator approach performs well in generating ensemble of precipitation and temperature, as well as, in capturing the annual dynamics and variability of the climate variables. From the 1000 generated precipitation and temperature time series values, 100 of them were selected using correlation and variability of their extreme values. Interestingly, spread of the correlation values of Gaoshiyo, Hinjiuma and Fustvatn catchments are significantly wider and it may have a clear impact on the uncertainty band of extreme flow (Figure 3A). Meanwhile, the spread of temperature values is not significantly changed within the sample (Figure 3B). This implies that precipitation has relatively higher variability in terms of magnitude and intensity, while temperature is not significantly varied in the given period.

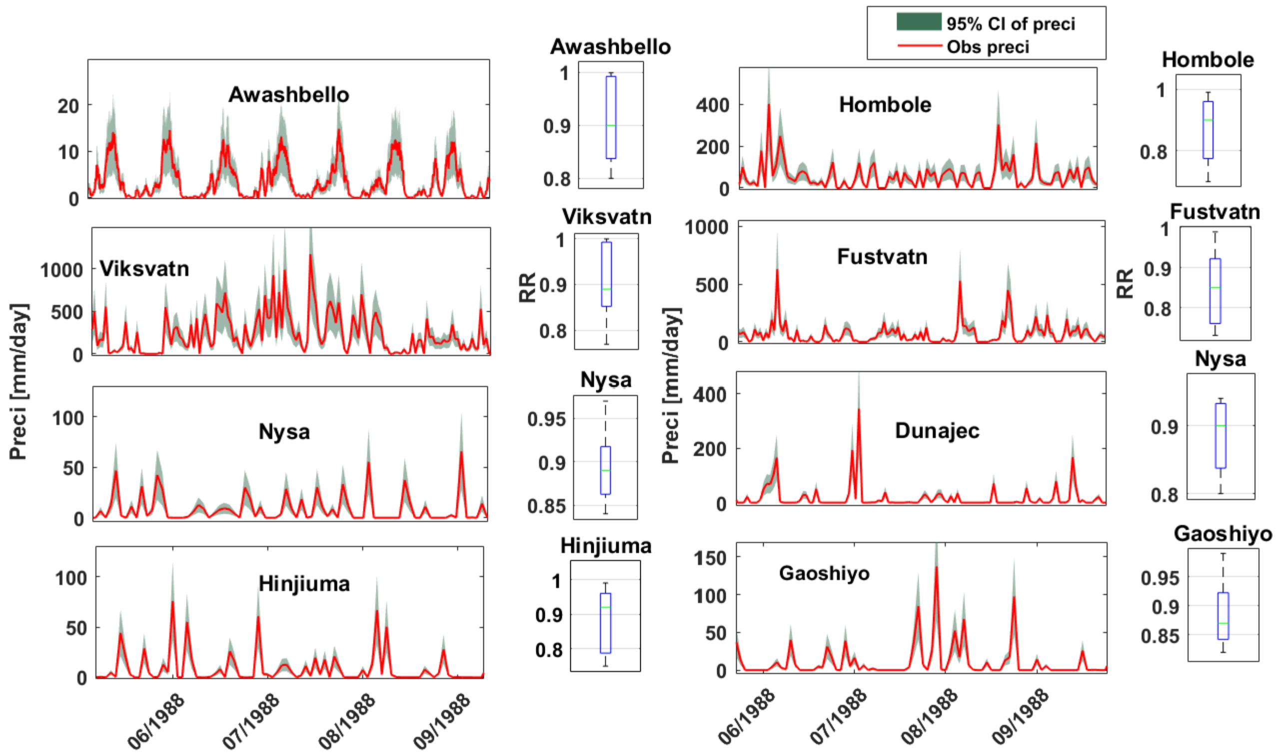

Figure 3A. Scatter representation of 1000 generated precipitation time series correlation value with maximum and average observed precipitation for eight sub-catchments. Each red or blue dote represents individual maximum and average precipitation simulation, respectively. The time period of each sub-catchment is presented in Table 1.

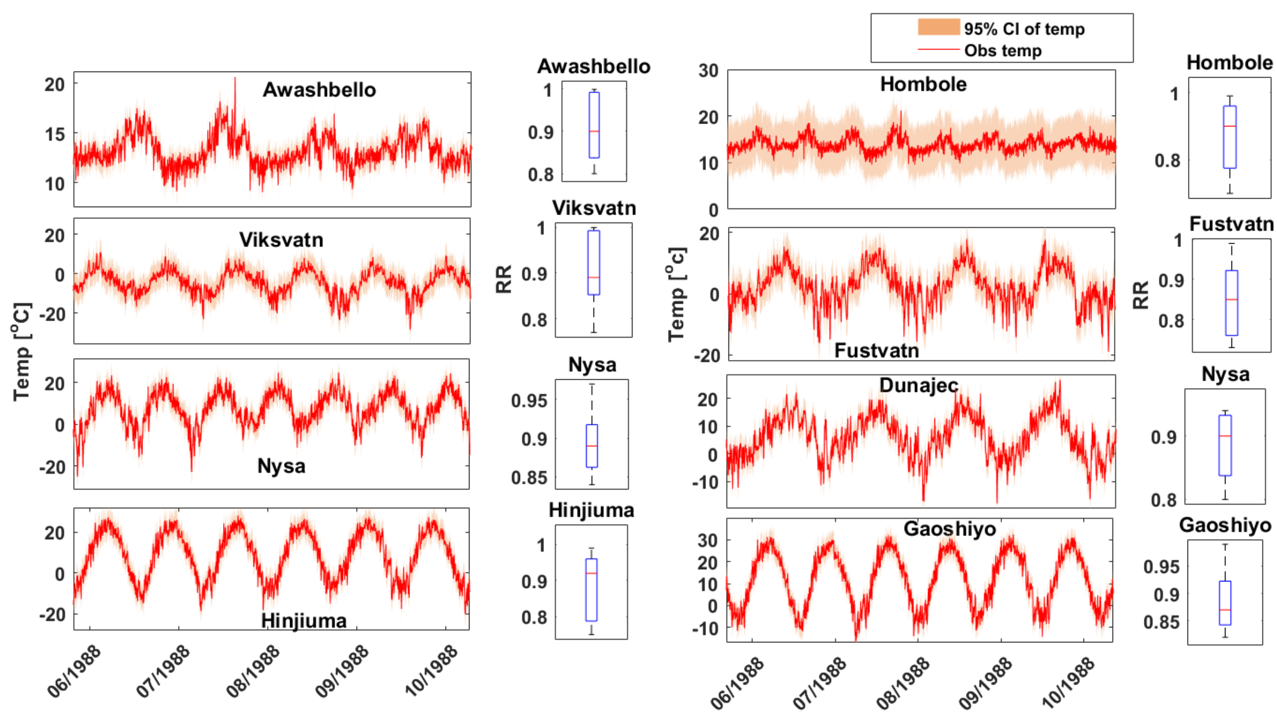

Figure 3B. Scatter representation of 1000 generated temperature time series correlation value with maximum and average observed temperature for eight sub-catchments. Each red or blue dot represents individual maximum and average temperature simulation, respectively. The time period of each sub-catchment is presented in Table 1.

4.2 Hydrological simulations

In order to ultimately capture the extreme streamflow predictions, two objective functions were used., The NSE for extreme high streamflow prediction and LogNSE is for extreme low flow were used to separate the most behavioral parameter sets from the lower one. Figure 4 presents the results of best 100 hydrological parameter sets and their respective weights using XAJ, HBV and GR8J hydrological models. The LogNSE and NSE results are not one to one related sets and had not significant correlation. This confirms that each hydrological regime governed by different hydrological parameter values. The simulated extreme hydrological flow using these NSE and LogNSE values were used further for hydrological parameter uncertainty investigation. The result of median of each objective function for each hydrological model was quite good and promising for uncertainty estimation. For example, the NSE value of Fustvaten, Dunajec, Hombole and Gaoshiyo is 0.8, 0.7, 0.67, and 0.6, respectively (Figure 3). The simulated extreme flow was weighted by NSE and LogNSE and produce quite high values for these 100 behaviour sets using XAJ, HBV and GR8J models (Figure 7). The average NSE of the three hydrological models is almost uniform across the catchments and produces above the minimum NSE threshold value. XAJ is relatively perform good in Hamoble and Awahsbello, whereas, GR8J model was explained the observed flow of Dunajec and Nysaklodska very well. This is likely due to model structure differences and number of parameters, such as the number of water storage reservoirs and flow generation mechanisms.

Overall, Figure 4 shows the results of three hydrological model performance with the application of MC sampling with GLUE and a bounded NSE and LogNSE objective functions for each catchment. The bounded likelihood function has more advantages to compare the results of hydrological models (Mathevet et al., 2006). Unlike, the NSE (one side bounded objective function), has fixed upper and lower boundaries ([-1 1]). The three hydrological models performed quite well to simulate river flow. However, the extreme flow simulation is very difficult, and the three hydrological models had a very wide range of NSE values. The mean NSE and LogNSE value of each catchment shows a reasonably acceptable value and feasible to understand the uncertainty in the catchments, keeping the varying results between the catchments. The uniform distribution sampling from the hydrological parameter ranges (Table 2) has its own impact on the simulated hydrological extremes.

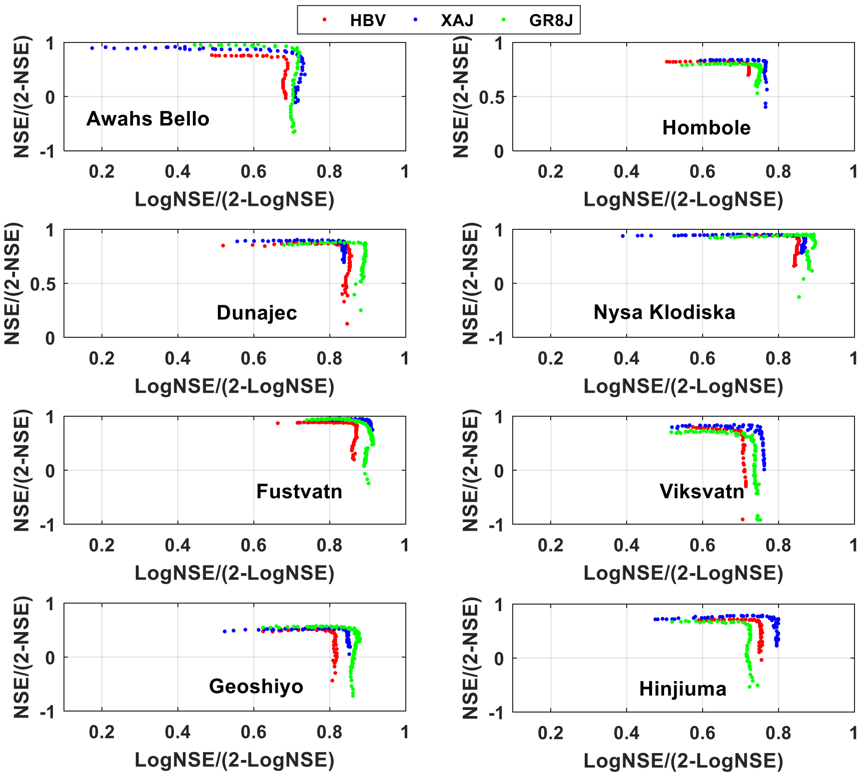

Figure 3. Bounded NSE for peak flow (left column) and LOGNSE for low flow evaluation (right column) results for eight catchments from best/behavioral simulations of GR8J (blue), HBV (red) and XAJ (green) models. The hydrological parameters of XAJ, HBV and GR8J models are one of the critical sources of uncertainty to river extreme flow simulations and evaluated using seasonal high and low flow indices. 95% CI of simulated extreme flow using three hydrological models are estimated to examine the extent to which hydrological parameter uncertainty caused on model simulation. The uncertainty associated with the hydrological parameters in the simulation of the extreme river flow data was estimated by applying the GLUE approach described in section 3.6, which was evaluated using seasonal extreme indices derived from daily river flow time series, and presented in Figure 5A (high flow) and Figure 5B (low flow). Figure 5A, B indicates temporal evolvement of hydrological parameter uncertainty and its band on simulation of extreme peak flow using XAJ (red band), GR8J (blue) and HBV (green).

Generally, from Figure 5 A, B, it is clearly seen that the three hydrological parameters sets were lacking to capture the extreme values characteristics and the very extreme low values. Particularly, Hunjium catchment has very high events and these models were lacking to simulate these peaks (Figure 5A). Similarly, Gaoshiyo and Awash Bello catchments are Ephemeral River and with prolonged dry season, the simulation of the low flow was not 100% in the 95% CI. Overall, the structure of the hydrological models may provide important information in estimation of uncertainty. This indicates that simulations of low flow in ephemeral catchments are very difficult due to their prolonged dry conditions. For the estimation of peak flows, the uncertainty comes from the observed time series characteristics (the number of events). For example, if the catchment has few extremes, the model gives smaller band, but few extremes fall outside the 95% CI band. A single model is not able to consider all the processes in a watershed. Therefore, there is no perfect and universally applicable hydrological model and estimation of the uncertainty is important to build confidence in extreme flow prediction.

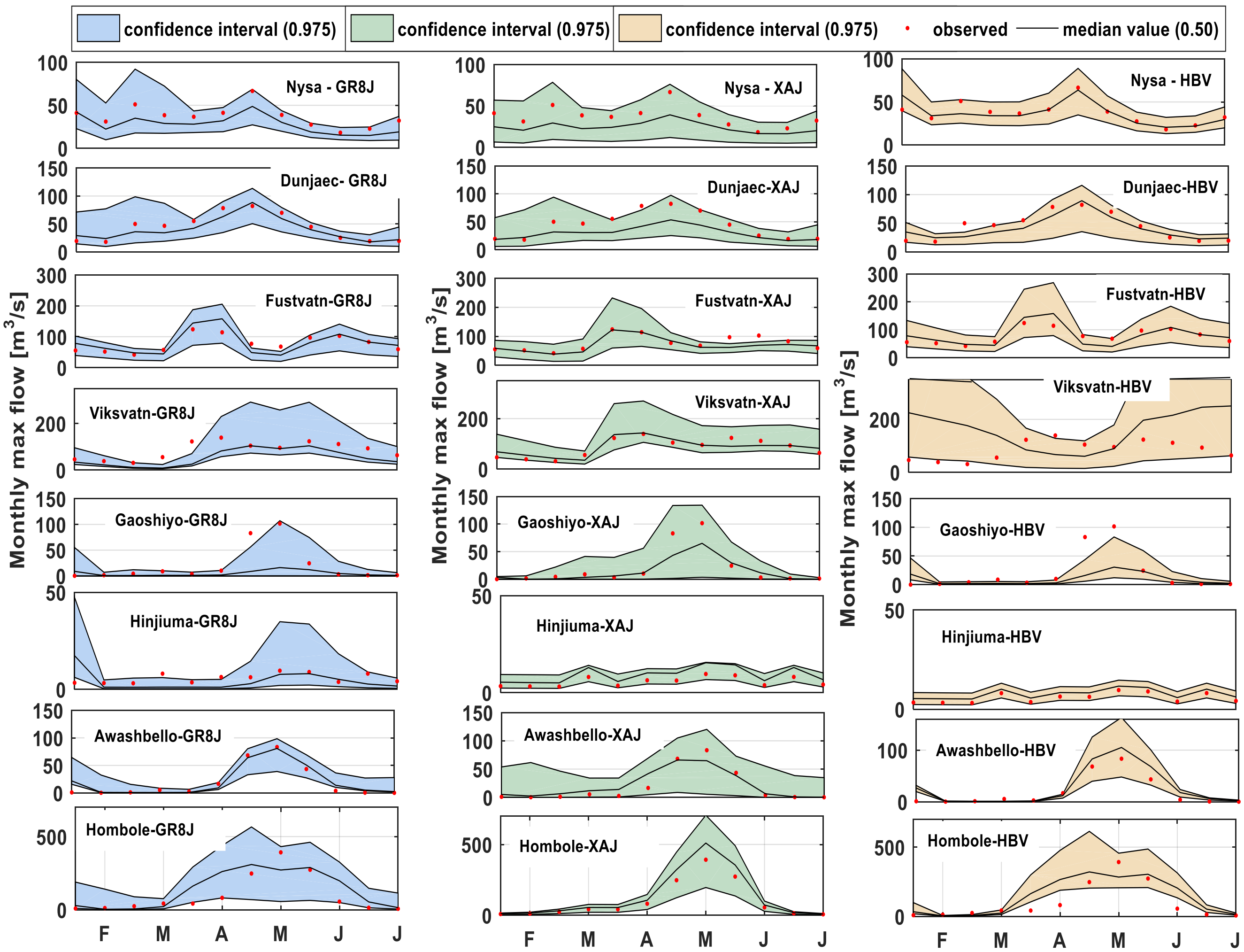

Figure 5A. Hydrological parameter uncertainty and its band on simulation of extreme monthly high flow using XAJ (green band), HBV (reddish) and GR8J (blue). Each color stands for the 95% confidence interval of 100 simulations from 100 best hydrological parameters. The red dot represents observed extreme maximum flow of respective stations.

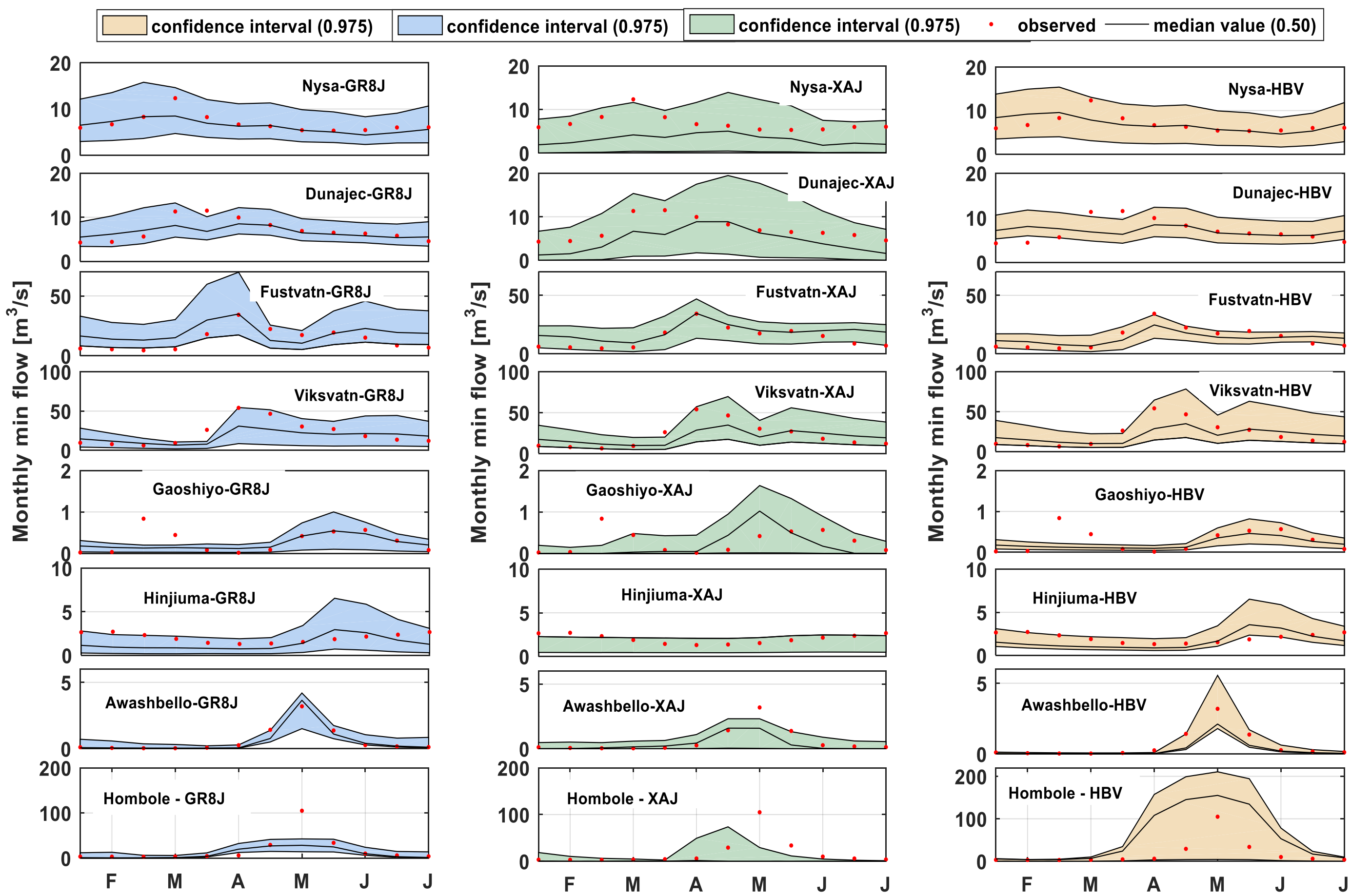

Figure 5B. Hydrological parameter uncertainty and its band on simulation of extreme monthly low flow using XAJ (green band), HBV (reddish) and GR8J (blue). Each color stands for the 95% confidence interval of 100 simulations from 100 best hydrological parameters. The red dot represents observed extreme minimum flow of respective stations.

4.3 Evaluation of temporal evolvement of hydrological model structure uncertainty

Figure 6A, B reveals simulated and observed peak flow and low flow of eight stations using three hydrological models for the given period. This shows the ensemble variability over time and has central line for mean of ensemble simulations from three hydrological model, fixed upper line of the ensample 95% and lower 5%, and shows the variability of the simulation compare to observed (blue broken lines) and temporal mean (Blue solid lines). Most of the extreme high flow are consistent and within the 95% (red line). This is affected by the temporal variation. Each box contains a result of GR8J, XAJ, HBV simulations, and the observed time series is presented with blue dotted line. The mean of the three hydrological models together is more comparable with the observed annual peak flow (Figure 6A) and low flow (Figure 6B) than the individual hydrological model simulation with observed flow time series. However, hydrological model uncertainty becomes much higher than the individual one. the models are failing to simulate two very big events in the Hinjiuma catchment and one large peak in the

Goashiyo catchment. In the Awash Bello catchment, the models are not able to produce observations due to the external forces like physiographic and ground water (Figure 6A). The remaining stations are almost reasonably fit with the median of these model simulations. In the low flow, the median of the simulation fit with the observed low flow except in the Goashiyo catchment. Except the Viksvatn and Nysaklodska catchments, the observed minimum flow is under the 95% fixed confidence interval (Figure 6B). the values are almost lies in the fixed mean value and reasonably comparable with observed low flow.

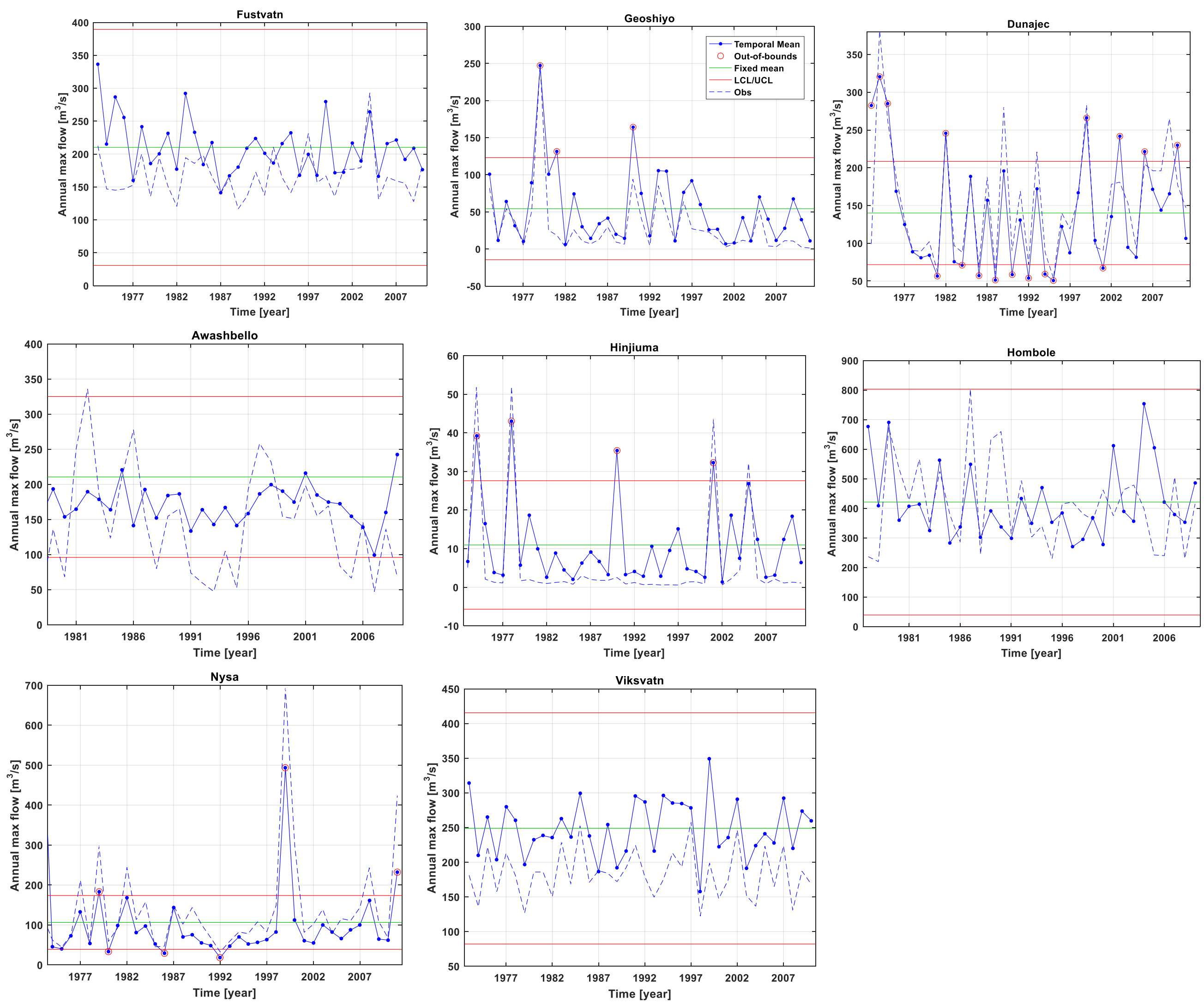

Figure 6A. Time evolution in hydrological model structure uncertainty. The upper and lower red lines represent the 95% confidence interval, blue solid indicates the ensemble median and broken blue line is the observed of extreme high flow simulation using three hydrological models (XAJ, HBV and GR8J), and green is the center of the 95 % confidence interval.

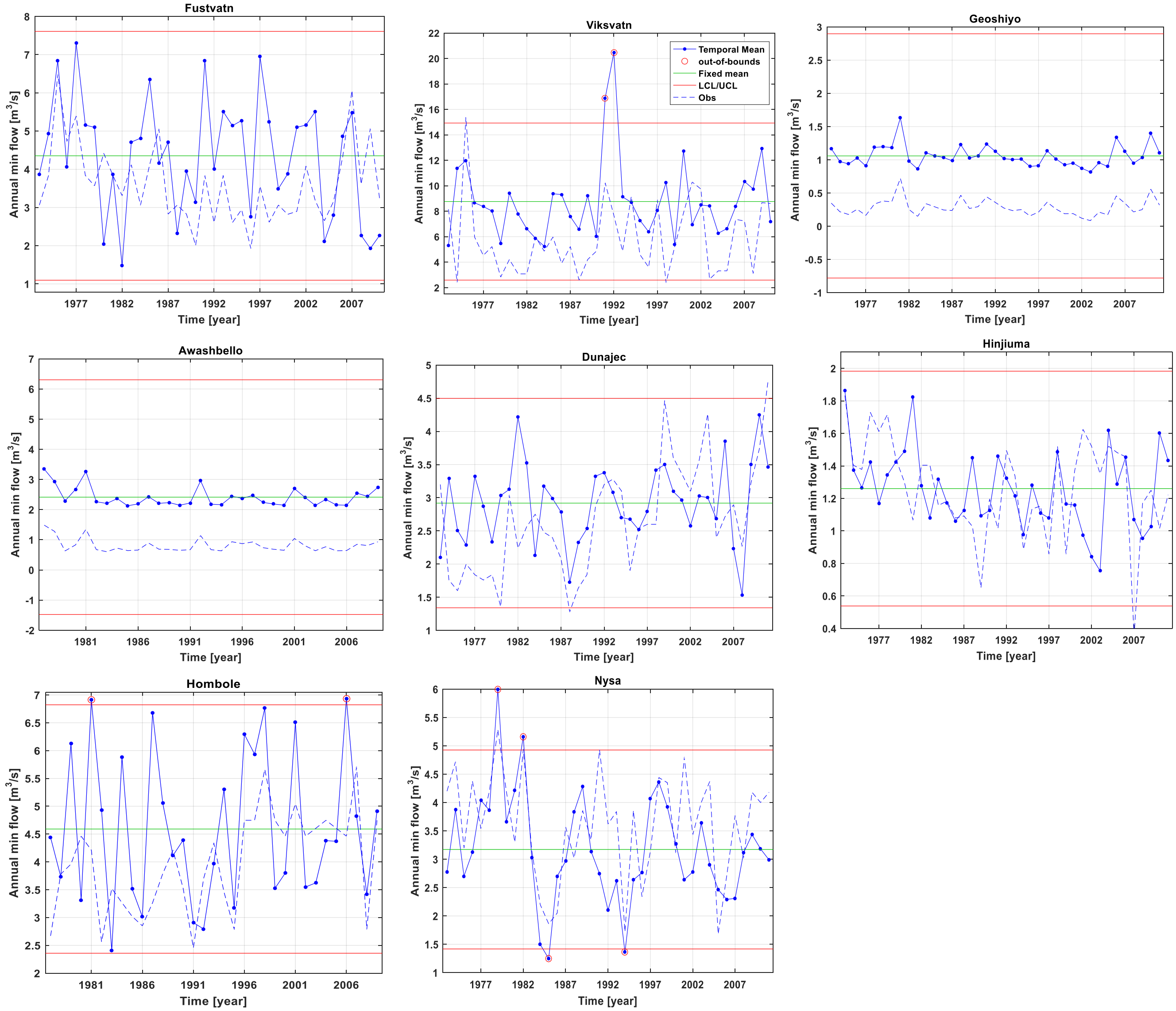

Figure 6B. Time evolution in hydrological model structure uncertainty. The upper and lower red lines represent the 95% confidence interval, blue solid indicates the ensemble median and broken blue line is the observed of extreme low flow simulation using three hydrological models (XAJ, HBV and GR8J), and green is the center of the 95 % confidence interval.

4.4 Evaluation of uncertainty propagation

The uncertainty that aggregated from the input data, hydrological model structure, hydrological parameters, and extreme frequency distribution models becomes larger and has significant implication in water resource and flood risk management. The total uncertainty increases as the number of sources of uncertainty increases in peak flow and low flow frequency estimation (Figure 7A, B). The potential impact of each source of uncertainty is estimated by comparing the 95% CI band in the extreme peak and low flow frequencies (Figure 7. A, B). Figure 6A, B, displays the total frequency curves of peak and low flow based on the given period. Each source of uncertainty presented by each color shade (the colors are additive): green represent extreme frequency models, orange color for input data, blue for hydrological models and pink color for hydrological parameters. Their corresponding median values are presented in solid lines of respective uncertainty bands color: red line, yellow line, blue line, and green line.

The additive way of total uncertainty presentation in Figure 7A, B does not illustrate both the main variables and their interaction uncertainty at the same time. It shows only the impact of the sources of uncertainty. The aggregated uncertainty source accounted significant differences in estimation of peak flow and low flow quantiles. In peak flow quantiles estimation at different return period, the input data uncertainty band is higher than other sources of uncertainty. hydrological parameters have a larger impact on estimation of low flow frequency values. This implies that high quality input data is important to reduce uncertainty in water resource management (Figure 7A); and parameters and good structure of hydrological model play major role in the reliability and accuracy of environmental flow simulation (Figure 7B). This has a significant contribution for decision makers and water resource managers. Based on median of each sources of uncertainty deviation from total medium value, the extreme peak flow frequency mainly influenced by the uncertainty that come from the quality of the input data with 40% contribution to the total uncertainty, frequency distribution models contributed 30% to the total uncertainty, hydrological parameter sets contributed 20% and model structure 10% to the total uncertainty(Figure 7A), in the modeling of low flow frequency, the contributors to the total uncertainty are ranked as parameter uncertainty (35%), hydrological model structure (28%), quality of input data (25%) and frequency distribution models (12%) (Figure 7B).

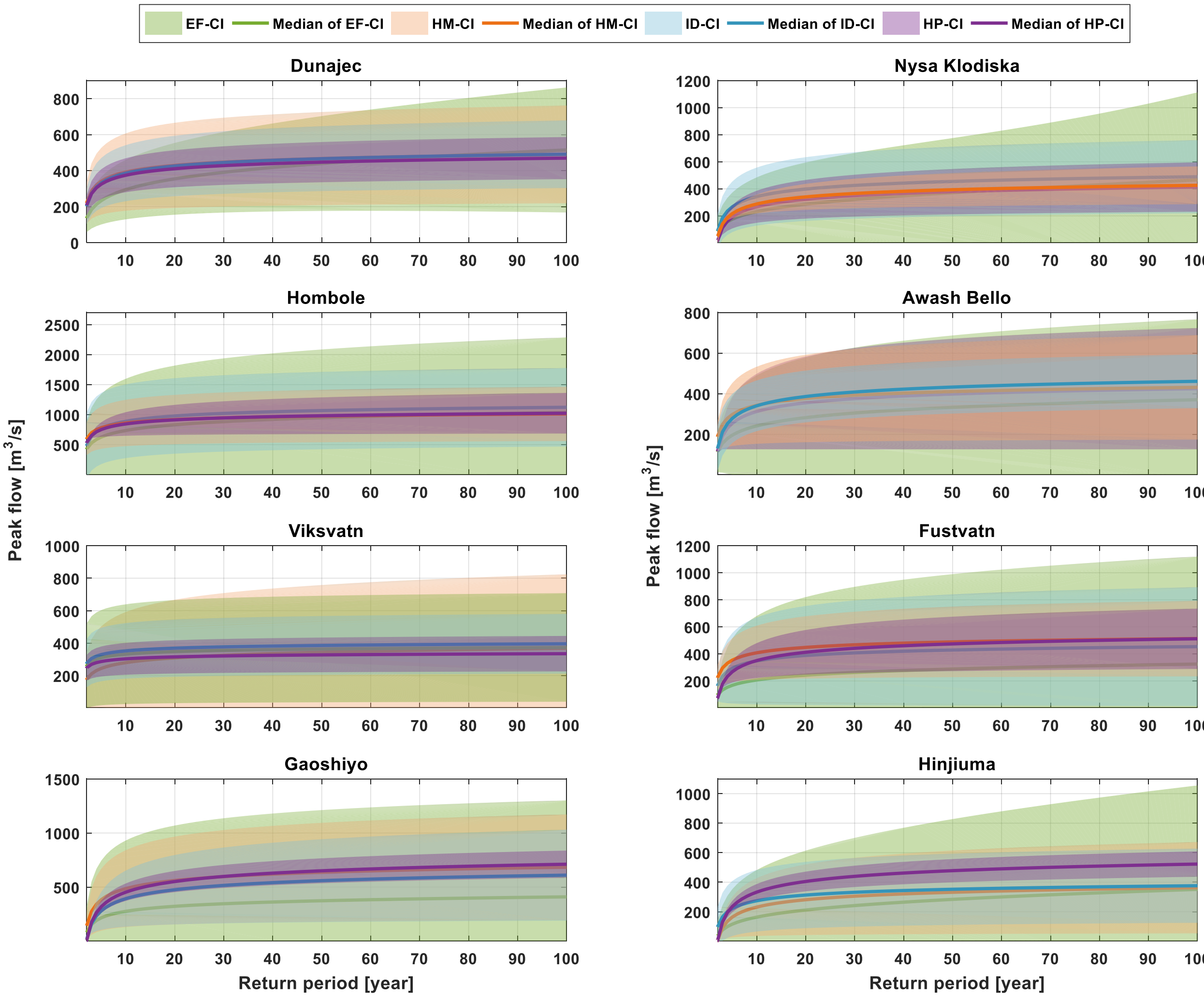

Figure 7A. Aggregated/total uncertainty of peak flow quantiles for eight catchments based on 30 years simulated data. These uncertainties are related to four main variables: input data (blue color), hydrological parameters (pink color), hydrological models (orange color) and extreme frequency distribution models (green color). The solid lines are median of the respective uncertainty bands: blue line, pink line, red line, and green line.

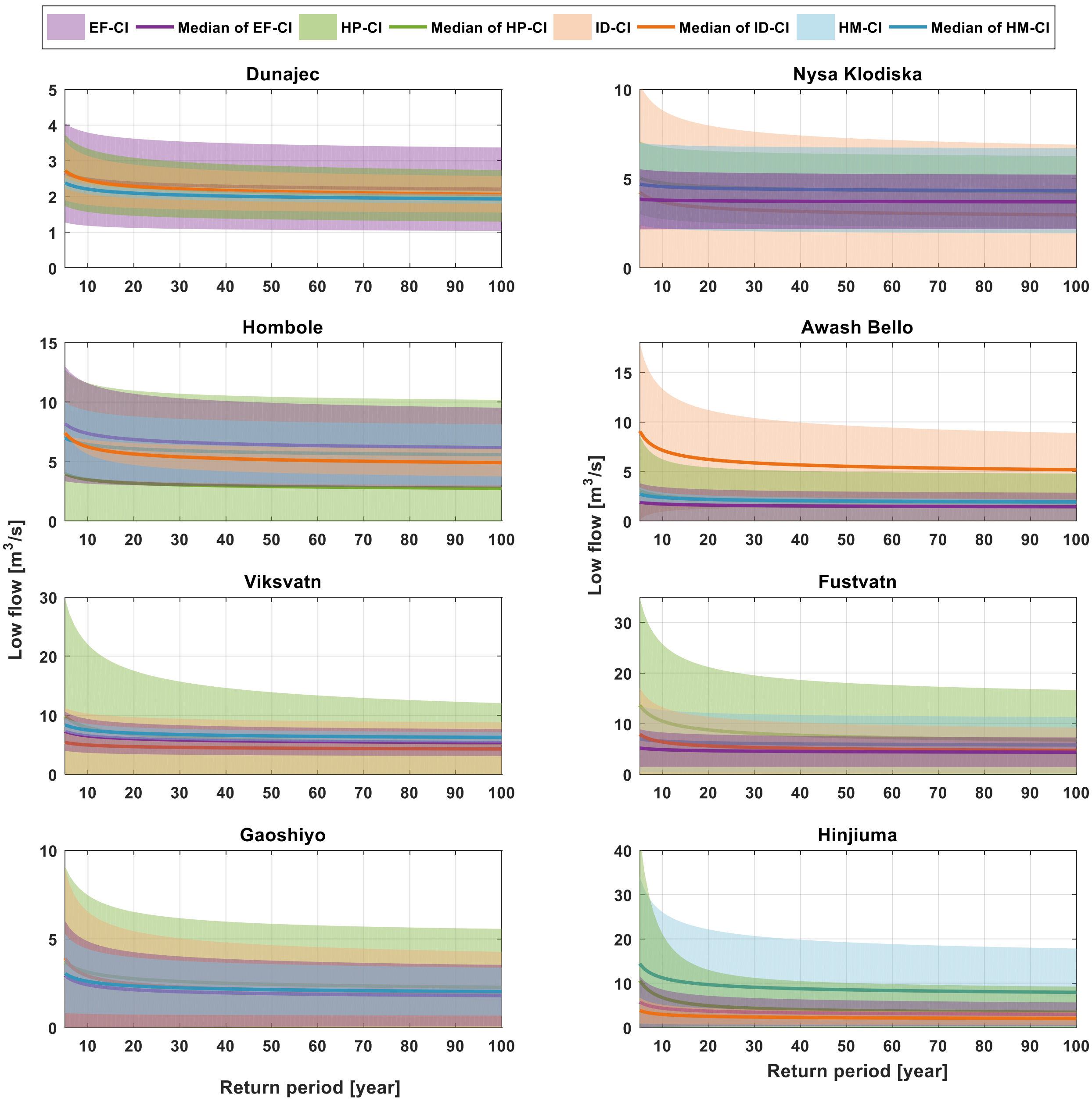

Figure 7B. Aggregated/total uncertainty of low flow quantiles for eight catchments based on 30 years simulated data. These uncertainties are related to four main variables: input data (orange color), hydrological parameters (green color), hydrological models (blue color) and extreme frequency distribution models (pink color). The solid lines are median of the respective uncertainty bands: red line, green line, blue line, and pink line.

4.5 Uncertainty decomposition using their variances

Variance based uncertainty decomposition is helpful to understand the interaction of the main sources of uncertainty. Figure 8A, B, shows the results of the variance decomposition and provides the percentile contribution of each variable and its interactions. For peak and low flow quantiles, four main variables and their interactions were identified using ANOVA. The low flow quantile at 10-year return period (QT10) and the peak flow quantile at 90-year return period (QT90) were considered for ANOVA analysis (Figure 8A, B). These values were derived from four main groups flow simulations and weighted by logNSE and NSE likelihood, respectively. The variance based sensitively analysis results presented in Figure 8A, B confirm our earlier results on the major influences of the input data spread on the magnitude of high flow quantile (QT90) and supreme influence of hydrological parameters on the magnitude of low flow quantile (QT10). Even though, Figure 7A, B and Figure 8A, B show that the main variables have a huge impact on the estimation of low flow frequency and peak flow frequency at different return period, but at the same time, the interaction of these variables also played significant role to the total uncertainty band. In particular, the interaction of input data band and extreme frequency models band have significant influence on peak flow quantile values. Similarly, the interaction of hydrological models and hydrological model parameters have big role on low flow quantile estimation. The ANOVA analysis result also confirms that inter-dependency of these four sources of uncertainty is high and should be considered in water resource modeling and in flood risk management.

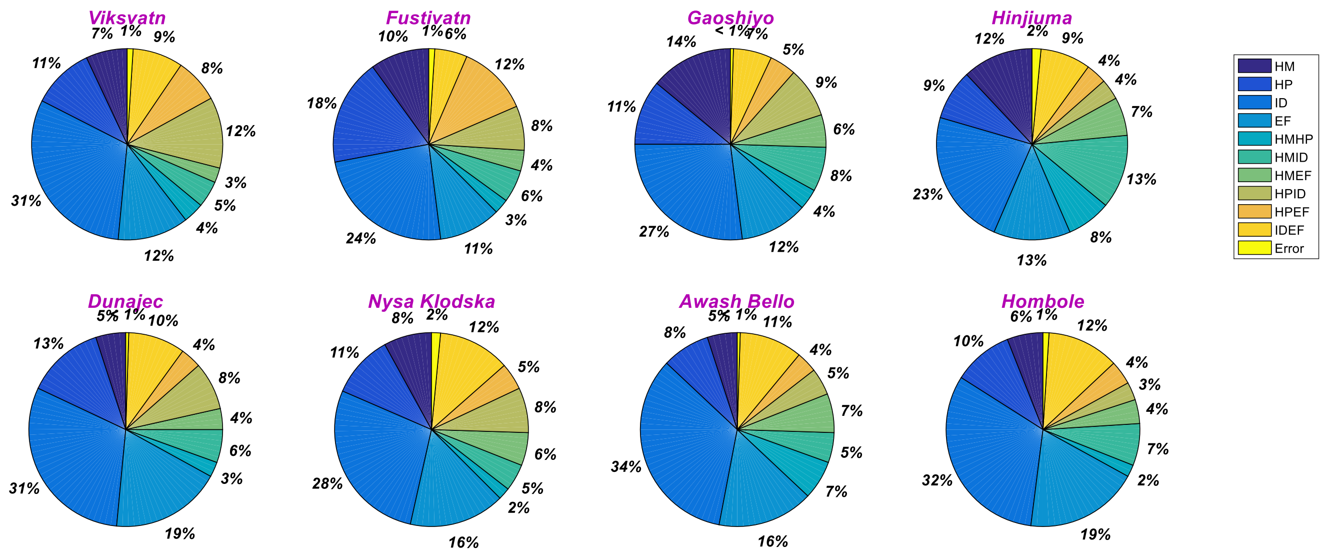

Figure 8A. the shares of uncertainty related to HM-hydrological models, HP-hydrological parameters, ID-input data, EF-extreme frequency and their interaction terms (HMHP-hydrological models and hydrological parameters, HMID- hydrological models and input data, HMEF- hydrological models and extreme frequency, IDEF-input data and extreme frequency) for the selected eight catchments at QT90 (extreme peak flow quantile at 90 years return period).

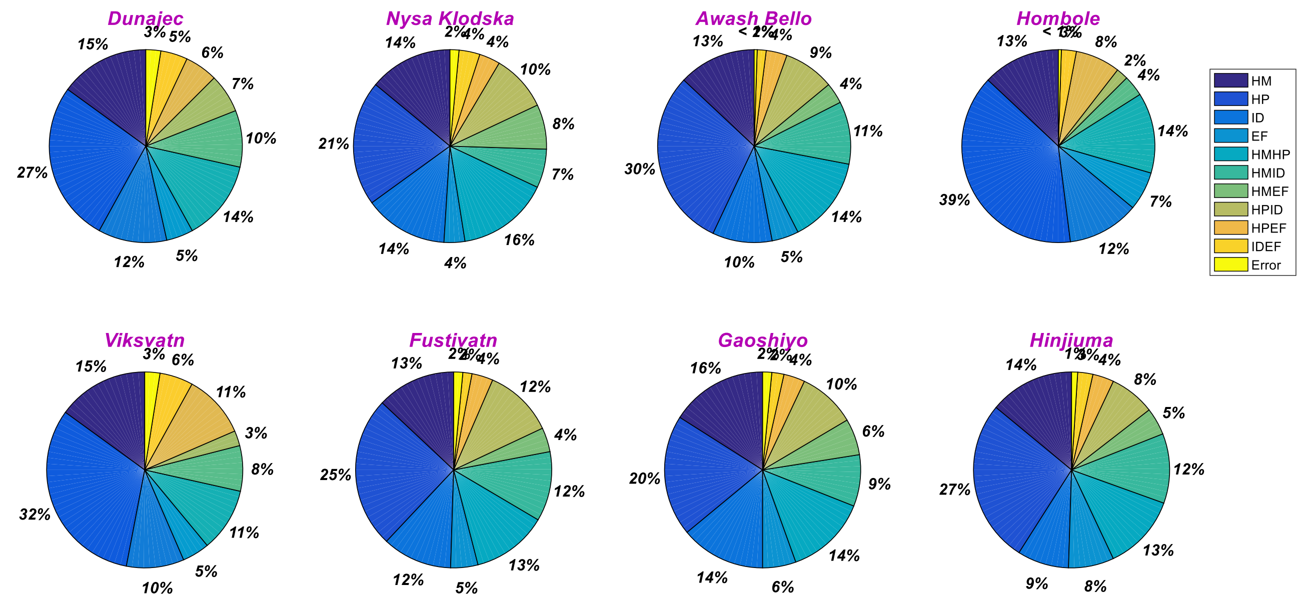

Figure 8B. the shares of uncertainty related to HM-hydrological models, HP-hydrological parameters, ID-input data, EF-extreme frequency and their interaction terms (HMHP-hydrological models and hydrological parameters, HMID- hydrological models and input data, HMEF- hydrological models and extreme frequency, IDEF-input data and extreme frequency) for the selected eight catchments at QT10 (extreme low flow quantile at 10-year return period).

5. Discussion

This study demonstrates the importance of uncertainty propagation quantification and understanding for extreme river flow simulations and its frequency at different return periods. The associated uncertainty in extreme frequently modeling is varied and depends on the catchment characteristics, adequacy and quality of forcing data, flow regime, choice of model and parameterization approach.

This framework is new and highly proposed to quantify the uncertainty propagation from input to frequency of floods and hydrological droughts. A Gaussian distribution model with a specific mean and standard deviation was used to generate realizations of precipitation time series data. This error term was multiplied with the observed precipitation time series data to get the possible realization of precipitation values. Temperature data were generated using mean and standard deviation of observed temperature data by adding or error term to observed temperature time series. Both generated realizations of precipitation and temperature time series were used as input to three hydrological models to estimate the role of input data time series uncertainty on extreme flows.

Different types of sources of uncertainty associated to extreme flow frequency were identified in order to compare and characterize their impact on the quantity of extreme flow. In this framework, ensembles of precipitation and temperature data, three hydrological models, ensembles of hydrological parameter sets and five extreme frequency models were applied in order to understand the uncertainty propagation from each component.

Eight study areas were selected from four countries with different flow regime, catchment characteristics and hydro-climate conditions to evaluate the uncertainty propagation framework under different pre-conditions. The sources of uncertainty were evaluated using extreme low flow frequency and extreme high flow frequency at different return periods; these two main variables were defined as main hydrological indicators.

5.1 Uncertainty propagation and robustness of the approach

Associated sources of uncertainty in flood and low flow frequency magnitude are quantified. The input uncertainty was established using the generated realization of precipitation and temperature to address the reliability of hydrological simulations. This is a simple and feasible approach in improving hydrological simulations. Ajami et al. (2007) also used similar way of input uncertainty estimation, but the concept of the model was only applied for precipitation variable under unknown mean and variance, which may lead to bias in sampling and unrealistic ensembles. the accuracy of generated ensembles was demonstrated by capturing the observed maximum precipitation and temperature time series (Figure 3A, B). The generated realization of climate data was better in Viksvatn and Awashbello than the others. This is related to their less maximum precipitation events and dry spell length. If the spread of generated precipitation and temperature realization is wide, it will be transferred to the extreme flow, resulting in the wide range in peak or low flow extremes.

The results of input data uncertainty were evaluated using three hydrological models for eight catchments (Figure 4) and 100 best input data. The uncertainty range due to input data is presented within the box plot for each catchment. In high flow, the three hydrological models show relatively similar band of 75% and 25% of both plot range. In the low flow simulations, the HBV model has a wider band than the other two hydrological models (Figure 4). This indicates that simulations of low flow of ephemeral catchments are very difficult due to their prolonged dry conditions. In estimation of peak flows, the main difficulty comes from the observed time series characteristics (the number of peak or low events). For example, if the catchment has few extremes, the model gives a smaller band, but few extremes fall outside of the band. Tian et al. (2013) compared XAJ, HBV and GR4J hydrological models for climate change impact study in China and found similar results as presented in this study. Meresa and Gatachew, (2018) also compared three hydrological models (GR4J, HBV and HMETS) for climate change impact assessment in Ethiopia and found significant differences.

The hydrological parameter uncertainty was estimated using GLUE, which is straight forward and frequently used in parameter uncertainty estimation in hydrology. In addition to the input data and hydrological model uncertainty, hydrological parameter sets have very significant contributions to the extreme flow frequency. Similarly, Yen et al. (2018); Meresa and Romanowicz, (2017); Bae et al. (2018) also found that the contribution of parameter uncertainty is significant as presented in this study. However, the role of hydrological parameter sets is not the same for all flow regimes. The peak flow is less influenced by parameters than the low flow. This is because of the model parameters that governs the slow and fast flow components of the hydrological water balance. The peak flow component is highly influenced by the snow and soil surface layer related parameters, while low flow magnitude is controlled by the snow, surface and sub-surface soil related parameters (Figure 5A, B). Overall, the three hydrological models showed consistent results and near to the observed peak flow. low flow simulations band value is not fitted to observed low flow values. This is most likely due to the influence of physiographic features in the hydrological cycle components (Zhang et al., 2016).

In water resource and flood risk management practical exercise, it is mandatory to estimate the peak or low flow frequency using a statistical distribution. However, estimates depend on the extreme distribution model (Sun et al., 2017). Hydrological and statistical approaches were combined to estimate the frequency of extreme low and peak flow at eight catchments. The result confirms that the frequency distribution uncertainty range (from five distribution types) also significant contributes to the flood design magnitude. Okoli, (2019) found a similar result. These sources of uncertainty play a major role in water resource management and planning, food security, flood risk reduction, poverty reduction and bio-diversity conservation.

In this study, one-line chain from the input to the frequency magnitude of extreme flow at different return period and total variance-based approach uncertainty decomposition was deployed (Figure 7A, B and 8A, B, respectively). The results of variance-based analysis showed that input uncertainty has a larger contribution to the peak flow frequency magnitude at different return periods. However, using variance-based decomposition (ANOVA), the second large contributor is the interaction term of input data and extreme frequency model. Whereas, using one-line chain, the second large contributor is extreme frequency model. This is due to lack of consideration of the interaction effect in the one line chain uncertainty decomposition approach; at the same time, it is also visible that the ANOVA has an advantage by considering the interaction effect. Similarly, Meresa and Romanowicz, (2017),and Sun et al. (2017) also found the same result. Therefore, these results are associated with the case study areas considered here; however, the framework can be applied elsewhere to evaluate and examine uncertainty for extreme peak and low flow frequency estimation at different return periods.

The proposed comprehensive uncertainty propagation estimation approach is very important for decision makers and water resource managers. Especially, these results are very mandatory in flood risk modeling and extreme hazard estimation. Therefore, it would be an essential study, if researchers focus further on how these findings will propagate to risk and drought probability maps. This will be done by integrating these results with hydrodynamic model to investigate the uncertainty in flood risk and drought probability maps at different return periods.

5.2 Limitations of this framework

In this study, the nonstationary characteristics of the hydroclimate time series and models have not been considered. Therefore, care is needed to extrapolate the results of uncertainty propagation quantification to future or a different time period. If nonstationary analysis of hydrological parameter and frequency models considered, there are even larger individual uncertainty of both low and peak extremes than those presented.

In the last few decades, land use and climate change has been significantly changed, which may affect the characteristics of flow regimes, including excess flow and infiltration. Therefore, it is suggested, if further physical based hydrological model is considered to capture the range of flow dynamics.

6. Conclusions

This study demonstrates the importance of uncertainty propagation quantification in extreme river flow simulation and frequency at different return periods. The associated uncertainty in extreme frequently modeling depends on the catchment characteristics, adequacy and quality of forcing data, flow regime, choice of model and parameterization approach. Further, this newly developed framework is a good and comprehensive lesson that one can learn in extreme risk management and water resource management in most intermediate complexity catchments. Similarly, it helps to fix the problem of uncertainty estimation and consideration in practical exercises and natural resource management. The influence of uncertainty on the simulated flow is not uniform across all the selected catchments. Unsurprisingly, the uncertainty in modeling of extreme high flow frequency mainly comes from the quality of the input data, while in the modeling of low flow frequency, the main contributor to the total uncertainty is model parameter sets uncertainty. This result is also confirmed using ANOVA that adds additional information about the interaction of the main factors. The total uncertainty of QT90 quantile shows that the interaction of input data and extreme frequency models has significant influence on the total uncertainty. In the QT10 estimation, the hydrological models and hydrological parameters have a significant impact on the total uncertainty. In general, input data and its interaction with extreme distribution models are the main factors in modeling of extreme peak flow frequency for water resource management and flood risk management. Hydrological parameters and hydrological model structures are the most influential factors in low flow frequency estimation for environmental flow modeling and reservoir regulation. This implies that four of the main factors and their interaction may cause significant risk in water resource management and flood and drought risk management. Neglecting these four factors and their interactions may lead to underestimation of risk.

The methodology framework enhanced in the procedure for estimation of uncertainty and identification by giving a compressive overview and treat of possible sources of uncertainty in extreme (flood and drought) frequency magnitude. The results confirm that the framework is sufficient for flood risk managers and modelers, water resource managers, drought disaster risk managers, decision makers and ecologists; and it gives an outstanding overview and alarm what people should consider and follow.

Acknowledgements

This study is supported by the CAS Pioneer Talents Program and the National Natural Science Foundation of China (Grant No. 41971032). We thank anonymous reviewers and editors for their critical but constructive comments on this paper. We acknowledged the National Meteorological Agency (NMA) and Ethiopian Water Irrigation and electric city minister in Ethiopia for kindly providing the hydro-meteorological data of Ethiopia. Similarly, Institute of Meteorology and water resource management (IMWM) office for hydro-meteorological data of Poland. We extend our thanks to Jinkai Luan for kindly providing the hydro-meteorological data of China.

The data used in this study is available at https://github.com/hkmhkmhkm/HKdata.

Declaration of competing interest

The authors declare no conflicts of interest.

References

Ajami, N.K., Duan, Q., Sorooshian, S., 2007. An integrated hydrologic Bayesian multimodel combination framework : Confronting input , parameter , and model structural uncertainty in hydrologic prediction 43, 1–19. https://doi.org/10.1029/2005WR004745

Bae, D.H., Trinh, H.L., Nguyen, H.M., 2018. Uncertainty estimation of the SURR model parameters and input data for the Imjin River basin using the GLUE method. J. Hydro-Environment Res. 20, 52–62. https://doi.org/10.1016/j.jher.2018.05.001

Bergstrom, S., 1976. Development and application of a conceptual runoff model for Scandinavian catchments. SMHI RHO 7. Norrkoping, 134. Beven, K., 2007. Towards integrated environmental models of everywhere : uncertainty , data and modelling as a learning process 11, 460–467.

Beven, K., Binley, A., 2014. GLUE : 20 years on 5918, 5897–5918. https://doi.org/10.1002/hyp.10082

Beven, K., Binley, A., 1992. The future of distributed models : model calibration and uncerainty prediction 6, 279–298.

Blöschl, G., et al., 2019. Twenty-three unsolved problems in hydrology (UPH) – a community perspective 6667. https://doi.org/10.1080/02626667.2019.1620507

Breinl, K., Di, G., Girons, M., Hagenlocher, M., Vico, G., Rutgersson, A., 2017. Can weather generation capture precipitation patterns across different climates , spatial scales and under data scarcity ? 1–12. https://doi.org/10.1038/s41598-017-05822-y

Butts, M.B., Payne, J.T., Kristensen, M., Madsen, H., 2004. An evaluation of the impact of model structure on hydrological modelling uncertainty for streamflow simulation 298, 242–266. https://doi.org/10.1016/j.jhydrol.2004.03.042

Chen, X., Yang, T., Wang, X., Xu, C.Y., Yu, Z., 2013. Uncertainty Intercomparison of Different Hydrological Models in Simulating Extreme Flows. Water Resour. Manag. 27, 1393–1409. https://doi.org/10.1007/s11269-012-0244-5

Dams, J., Nossent, J., Senbeta, T.B., Willems, P., Batelaan, O., 2015. Multi-model approach to assess the impact of climate change on runoff. J. Hydrol. 529, 1601–1616. https://doi.org/10.1016/j.jhydrol.2015.08.023

Emam, A.R., Kappas, M., Fassnacht, S., Hoang, N., Linh, K., 2018. Uncertainty analysis of hydrological modeling in a tropical area using different algorithms 12, 661–671.

Feng, X., Cheng, W., Fu, B., Lü, Y., 2016. Science of the Total Environment The role of climatic and anthropogenic stresses on long-term runoff reduction from the Loess Plateau , China. Sci. Total Environ. 571, 688–698. https://doi.org/10.1016/j.scitotenv.2016.07.038

Griffis, V.W., Stedinger, J.R., 2007. Evolution of Flood Frequency Analysis with Bulletin 17 283–297.

Hamon, W.R., 1963. Computation of direct runoff amounts from storm rainfall. internaltional association of hydrology publication, 63, 52-62.

He, S., Guo, S., Liu, Z., Yin, J., Chen, K., and Wu, X., 2018b. Uncertainty analysis of hydrological multi-model ensembles based on CBP-BMA method Shaokun He , Shenglian Guo , Zhangjun Liu , Jiabo Yin , Kebing Chen 1636–1651. https://doi.org/10.2166/nh.2018.160

Her, Y., Yoo, S.H., Cho, J., Hwang, S., Jeong, J., Seong, C., 2019. Uncertainty in hydrological analysis of climate change: multi-parameter vs. multi-GCM ensemble predictions. Sci. Rep. 9, 1–22. https://doi.org/10.1038/s41598-019-41334-7

Hu, Y., Liang, Z., Li, B., Yu, Z., 2013. Uncertainty Assessment of Hydrological Frequency Analysis Using Bootstrap Method 2013.

Jiang, S., Ren, L., Xu, C., Liu, S., Yuan, F., and Yang, X., 2018a. Quantifying multi-source uncertainties in multi-model predictions using the Bayesian model averaging scheme Shanhu Jiang , Liliang Ren , Chong-Yu Xu , Shuya Liu , Fei Yuan 954–970. https://doi.org/10.2166/nh.2017.272

Jin, X., Xu, C.Y., Zhang, Q., Singh, V.P., 2010. Parameter and modeling uncertainty simulated by GLUE and a formal Bayesian method for a conceptual hydrological model. J. Hydrol. 383, 147–155. https://doi.org/10.1016/j.jhydrol.2009.12.028

Jones, P.D., Harpham, C., Briffa, K.R., 2013. Lamb weather types derived from reanalysis products 1139, 1129–1139. https://doi.org/10.1002/joc.3498

Karakoram, C., 2016. Predictive Uncertainty Estimation on a Precipitation and Temperature Reanalysis Ensemble for Shigar. https://doi.org/10.3390/w8060263

Kavetski, D., Kuczera, G., Franks, S.W., 2006. Bayesian analysis of input uncertainty in hydrological modeling : 1 . Theory 42, 1–9. https://doi.org/10.1029/2005WR004368

Khazaei, M.R., Ahmadi, S., 2013. A new daily weather generator to preserve extremes and low-frequency variability 631–645. https://doi.org/10.1007/s10584-013-0740-5

Kiang, J.E., Gazoorian, C., Mcmillan, H., Coxon, G., Coz, J. Le, 2018. A Comparison of Methods for Stream fl ow Uncertainty Estimation. https://doi.org/10.1029/2018WR022708

Kidd, C., Huffman, G., 2011. Review Global precipitation measurement 353, 334–353. https://doi.org/10.1002/met.284

Krysanova, V., Vetter, Tobias, Eisner, S., Portmann, F.T., Döll, P., Hattermann, F.F., Vetter, T, Breuer, L., Su, B., Daggupati, P., Donnelly, C., Fekete, B., Fl, F., n.d. Sources of uncertainty in hydrological climate impact assessment : a cross-scale study OPEN ACCESS Sources of uncertainty in hydrological climate impact assessment : a cross-scale study.

Kusangaya, S., Warburton, M.L., Archer, E., Garderen, V., 2018. Evaluation of uncertainty in capturing the spatial variability and magnitudes of extreme hydrological events for the uMngeni catchment , South Africa. J. Hydrol. 557, 931–946. https://doi.org/10.1016/j.jhydrol.2018.01.017

Li, L., Xu, C., Xia, J., Engeland, K., Reggiani, P., 2011. Uncertainty estimates by Bayesian method with likelihood of AR (1) plus Normal model and AR (1) plus Multi-Normal model in different time-scales hydrological models 406, 54–65. https://doi.org/10.1016/j.jhydrol.2011.05.052

Madsen, H., Lawrence, D., Lang, M., Martinkova, M., and Kjeldsen, R., 2013. A review of applied methods in Europe for flood-frequency analysis in a changing environment. NERC/Centre for Ecology & Hydrology, 180pp. (ESSEM COST Action ES0901). Marton, D., Paseka, S., 2017. Uncertainty Impact on Water Management Analysis of Open Water Reservoir. https://doi.org/10.3390/environments4010010

Mathevet, T., Michel, C., Andréassian, V., Perrin, C., 2006. A bounded version of the Nash-Sutcliffe criterion for better model assessment on large sets of basins 211–219.

Mcmillan, H., Jackson, B., Clark, M., Kavetski, D., Woods, R., 2011. Rainfall uncertainty in hydrological modelling : An evaluation of multiplicative error models. J. Hydrol. 400, 83–94. https://doi.org/10.1016/j.jhydrol.2011.01.026

Meresa, H.K., 2019. River flow characteristics and changes under the influence of varying climate conditions. Nat. Resour. Model. https://doi.org/10.1111/nrm.12242

Meresa, H.K., Gatachew, M.T., 2018. Climate change impact on river flow extremes in the Upper Blue Nile River basin. J. Water Clim. Chang. jwc2018154. https://doi.org/10.2166/wcc.2018.154

Meresa, H.K., Romanowicz, R.J., 2017. The critical role of uncertainty in projections of hydrological extremes. Hydrol. Earth Syst. Sci. 21. https://doi.org/10.5194/hess-21-4245-2017

Meresa, H.K., Romanowicz, R.J., Napiorkowski, J.J., 2017. Understanding changes and trends in projected hydroclimatic indices in selected Norwegian and Polish catchments. Acta Geophys. 65, 829–848. https://doi.org/10.1007/s11600-017-0062-5

Mockler, E M, Chun, K.P., Sapriza-azuri, G., Bruen, M., Wheater, H.S., 2016. Advances in Water Resources Assessing the relative importance of parameter and forcing uncertainty and their interactions in conceptual hydrological model simulations. Adv. Water Resour. 97, 299–313. https://doi.org/10.1016/j.advwatres.2016.10.008

Mockler, Eva M., O'Loughlin, F.E., Bruen, M., 2016. Understanding hydrological flow paths in conceptual catchment models using uncertainty and sensitivity analysis. Comput. Geosci. 90, 66–77. https://doi.org/10.1016/j.cageo.2015.08.015

Okoli, K.M., Maurizio, B. Korbinian, and G. Di. Baldassarre., 2019. A systematic comparison of statistical and hydrological methods for design fl ood estimation Kenechukwu Okoli , Maurizio Mazzoleni , Korbinian Breinl 1665–1678. https://doi.org/10.2166/nh.2019.188

Perrin, C., Michel, C., Andre, V., 2003. Improvement of a parsimonious model for streamflow simulation 279, 275–289. https://doi.org/10.1016/S0022-1694(03)00225-7

Prein, A.F., 2019. Can We Constrain Uncertainty in Hydrologic Cycle Projections ? Geophysical Research Letters 3911–3916. https://doi.org/10.1029/2018GL081529

Qi, W., Zhang, C., Fu, G., Zhou, H., 2016a. Quantifying uncertainties in extreme flood predictions under climate change for a medium-sized basin in northeast China Quantifying Uncertainties in Extreme Flood Predictions under Climate Change for a Medium-Sized Basin in Northeastern China. https://doi.org/10.1175/JHM-D-15-0212.1

Qi, W., Zhang, C., Fu, G., Zhou, H., Liu, J., 2016b. Quantifying uncertainties in extreme flood predictions under climate change for a medium-sized basin in Northeastern China. J. Hydrometeorol. 17, 3099–3112. https://doi.org/10.1175/JHM-D-15-0212.1

Ren-jun, Z., 1992. The Xinanjiang model applied in China 135, 371–381.

Song, X., Zhang, J., Zhan, C., Xuan, Y., Ye, M., Xu, C., 2015. Global sensitivity analysis in hydrological modeling : Review of concepts , methods , theoretical framework , and applications. J. Hydrol. 523, 739–757. https://doi.org/10.1016/j.jhydrol.2015.02.013

Sun, H., Jiang, T., Jing, C., Su, B., Wang, G., 2017. Uncertainty analysis of hydrological return period estimation, taking the upper Yangtze River as an example. Hydrol. Earth Syst. Sci. Discuss. 1–26. https://doi.org/10.5194/hess-2016-566

Tian, Y., Xu, Y., Zhang, X., 2013. Assessment of Climate Change Impacts on River High Flows through Comparative Use of GR4J , HBV and Xinanjiang Models 2871–2888. https://doi.org/10.1007/s11269-013-0321-4

Vesely, F.M., Paleari, L., Movedi, E., Bellocchi, G., Confalonieri, R., 2019. Quantifying Uncertainty Due to Stochastic Weather Generators in Climate Change Impact Studies. Sci. Rep. 1–8. https://doi.org/10.1038/s41598-019-45745-4

Vetter, T., Reinhardt, J., Flörke, M., Griensven, A. Van, Hattermann, F., Seidou, O., Su, B., Vervoort, R.W., 2017. Evaluation of sources of uncertainty in projected hydrological changes under climate change in 12 large-scale river basins 419–433. https://doi.org/10.1007/s10584-016-1794-y

Vrugt, J.A., ter Braak, C.J.F., Clark, M.P., Hyman, J.M., Robinson, B.A., 2008. Treatment of input uncertainty in hydrologic modeling: Doing hydrology backward with Markov chain Monte Carlo simulation. Water Resour. Res. 44, 1–15. https://doi.org/10.1029/2007wr006720

WG4 : Flood frequency estimation methods and environmental change, n.d.

Winter, B., 2018. Sources of uncertainty in a probabilistic flood risk model. Nat. Hazards 91, 431–446. https://doi.org/10.1007/s11069-017-3135-5

Wu, L., Seo, D., Demargne, J., Brown, J.D., Cong, S., Schaake, J., 2011. Generation of ensemble precipitation forecast from single-valued quantitative precipitation forecast for hydrologic ensemble prediction. J. Hydrol. 399, 281–298. https://doi.org/10.1016/j.jhydrol.2011.01.013

Xu, L.L.C., 2014. The comparison of sensitivity analysis of hydrological uncertainty estimates by GLUE and Bayesian method under the impact of precipitation errors 491–504. https://doi.org/10.1007/s00477-013-0767-1

Xu, Y.P., Booij, M.J., Tong, Y. Bin, 2010. Uncertainty analysis in statistical modeling of extreme hydrological events. Stoch. Environ. Res. Risk Assess. 24, 567–578. https://doi.org/10.1007/s00477-009-0337-8

Yen, H., Wang, R., Feng, Q., Young, C., Chen, S., Tseng, W., Wolfe, J.E., White, M.J., Arnold, G., 2018. Input uncertainty on watershed modeling : Evaluation of precipitation and air temperature data by latent variables using SWAT 122, 16–26. https://doi.org/10.1016/j.ecoleng.2018.07.014

Zhang, C., Yan, H., Takase, K., Oue, H., 2016. Comparison of the Soil Physical Properties and Hydrological Processes in Two Different Forest Type Catchments 1 43, 225–237. https://doi.org/10.1134/S0097807816120034